Electronic Supplementary Information (ESI)

Improved Transport Properties and Novel Li Diffusion Dynamics in van der Waals C_2N/Graphene Heterostructure as Anode Materials for Lithium Ion Battery: A First Principles Investigation†

Yingchun Ding,[ac] Bing Xiao,[*b] Jiling Li,[c] Qijiu Deng,[c] Yunhua Xu,[c] Haifeng Wang[d] and Dewei Rao[*e]

[a]College of Optoelectronics Technology, Chengdu University of Information Technology, Chengdu, 610225, China
[b]State Key Laboratory of Electrical Insulation and Power Equipment & School of Electrical Engineering, Xi'an Jiaotong University, Xi'an , 710049, P.R. China
Email: bingxiao84@xjtu.edu.cn
[c]School of Materials Science and Engineering, Xi'an University of Technology, Xi'an 710048, China
[d]Department of Physics, College of Science, Shihezi University, Xinjiang, 832003, China
[e]School of Materials Science and Engineering, Jiangsu University, Zhenjiang 212013, P. R. China. E-mail: dewei@ujs.edu.cn

BoltzTraP method

The electrical transport properties were calculated using BoltzTrap code based on a semi-classic Boltzmann transport theory [1].

Under the approximation, the electrical conductivity and electric thermal conductivity as function of temperature T and chemical potential μ can be calculated from the following equations:

$$\sigma_{ij}(T,\mu)=\frac{1}{\Omega}\int g_{ij}(\xi)\left[-\frac{\partial f_{\mu}(T,\xi)}{\partial \xi}\right]d\xi \qquad (1)$$

Here e, Ω and ξ ε represent the electron charge, reciprocal space volume, and band energy, respectively. $\frac{\partial f_{\mu}(T,\xi)}{\partial \xi}$ is the differential of Fermi function. $g_{ij}(\xi)$ denotes transport distribution function, shown as

$$g_{ij}(\xi)=\frac{e^2}{N}\sum_{n,\vec{k}}\tau_{n,\vec{k}}v_i\left(n,\vec{k}\right)v_j\left(n,\vec{k}\right)\frac{\delta\left(\xi-\xi_{n,\vec{k}}\right)}{d\xi} \qquad (2)$$

where N is the k-points number in the entire BZ. $\xi_{n,\vec{k}}$ are the energy for n-th band at wave vector $\vec{k}$, $v_i\left(n,\vec{k}\right)$ is the corresponding velocity as defined as $v_i\left(n,\vec{k}\right)=\left(1/\hbar\right)\partial\xi_{n,\vec{k}}/\partial\vec{k}$ The relaxation time is treated as independence with n and $\vec{k}$ namely as a constant ($\tau_{n,\vec{k}}=\tau$). The electrical transport parameters were calculated based on the eigenvalues from PBE functional. To accurately predict the transport parameters, much denser k-mesh (20×20×1) was used for the integrations in 1st BZ.

[56] Madsen, G. K. H.; Singh, D. J. BoltzTraP. a code for calculating band-structure dependent quantities. Comp. Phys. Comm. 2006, 175, 67-71.

.

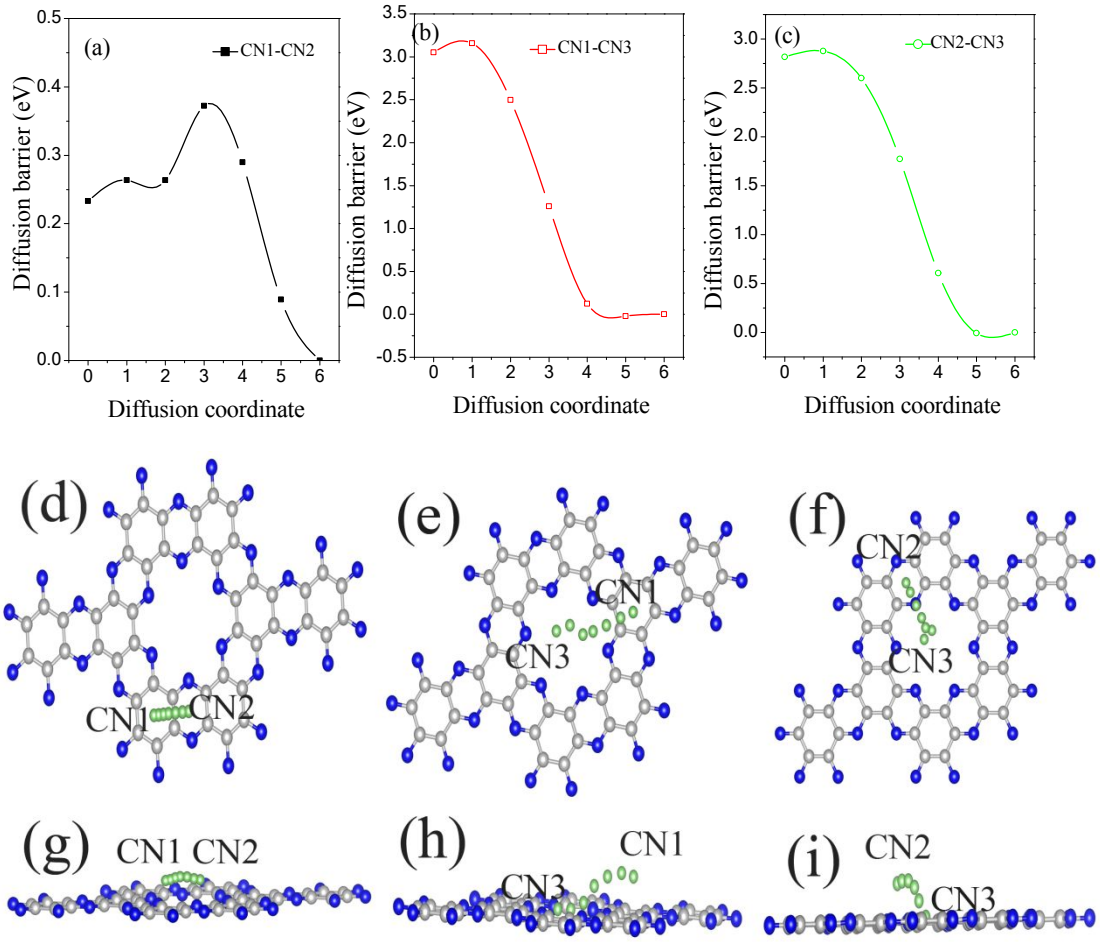

Fig. S1. The energy barrier of lithium diffusion pathways along the difference sites (top and side views) of 2D-C_2N.

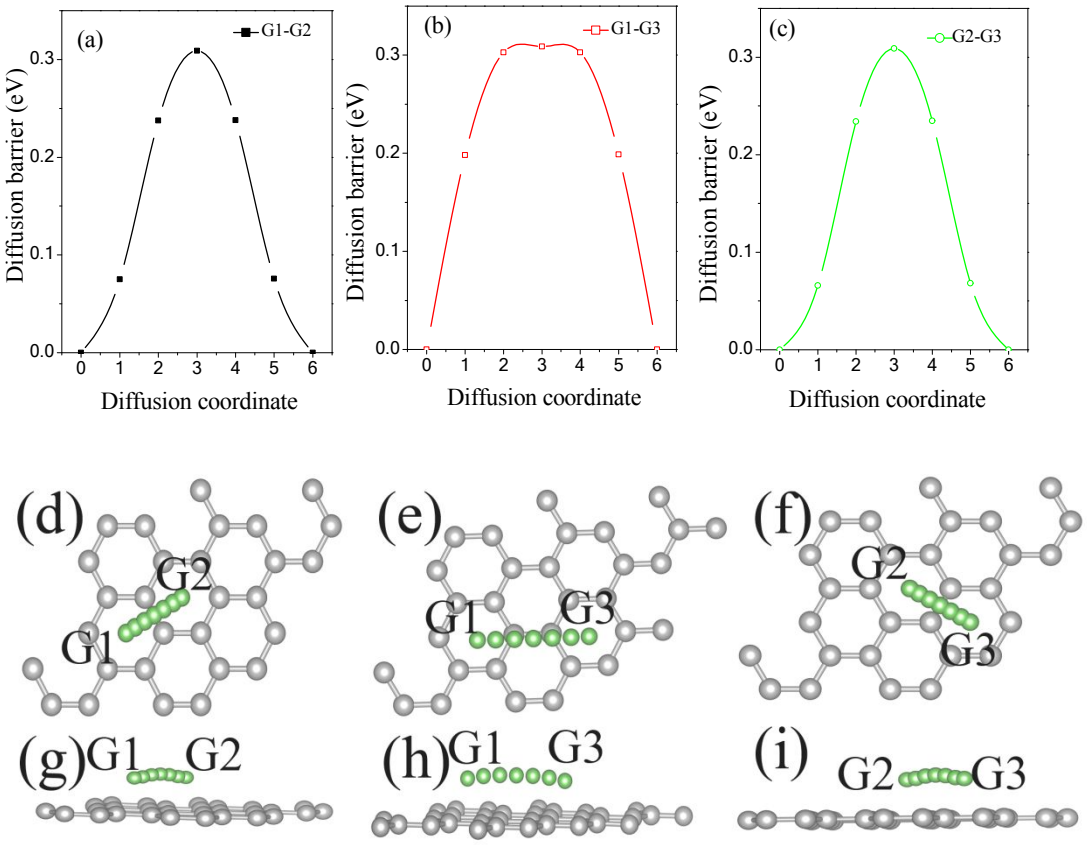

Fig. S2. The energy barrier of lithium diffusion pathways along the difference sites (top and side views) of Graphene.

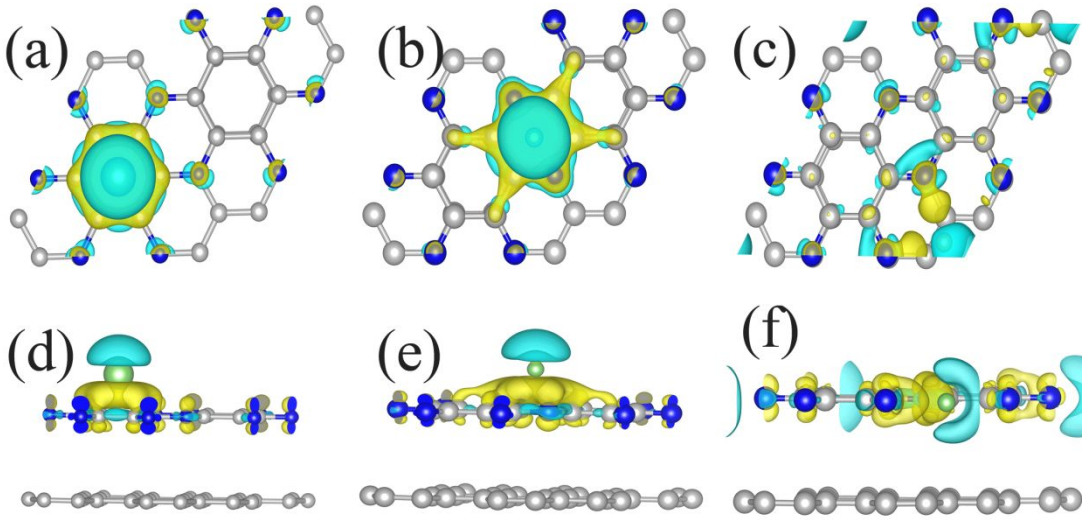

Fig. S3 The optimized structures and chosen adsorption sites (top of C_2N) of AA stacking for C_2N/G heterostructures. The charge density difference, $\Delta\rho$ (the top and side views) of Li-middle adsorption of C_2N/G heterostructure of AA stacking. The adsorbed in CN1(a, d),CN2(b, e) and CN3(c, f).

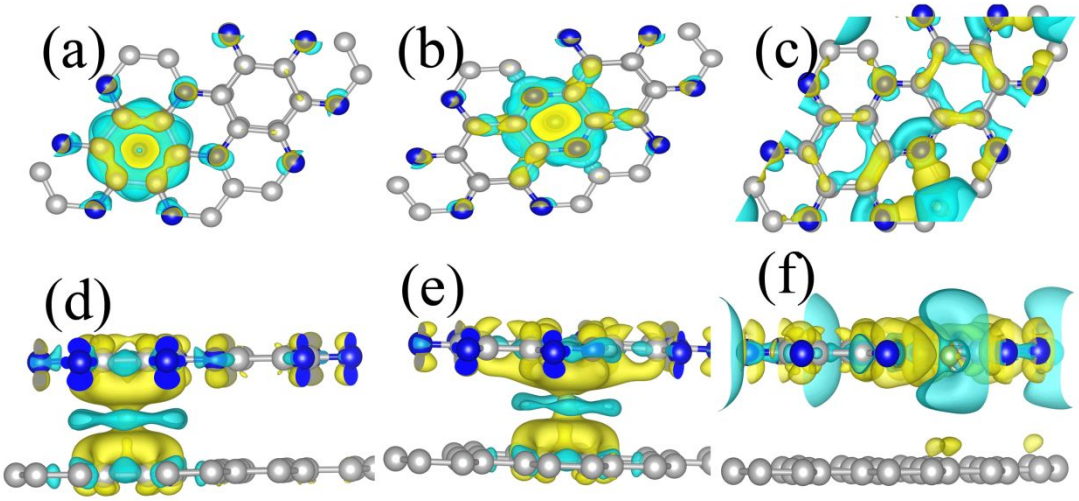

Fig. S4 The charge density difference, $\Delta\rho$ (the view) of Li-middle adsorption of 2D-C_2N/graphene heterostructure of AA stacking. The adsorbed GCN1 (a, e), GCN2 (b, f) and GCN3 3(c, g).

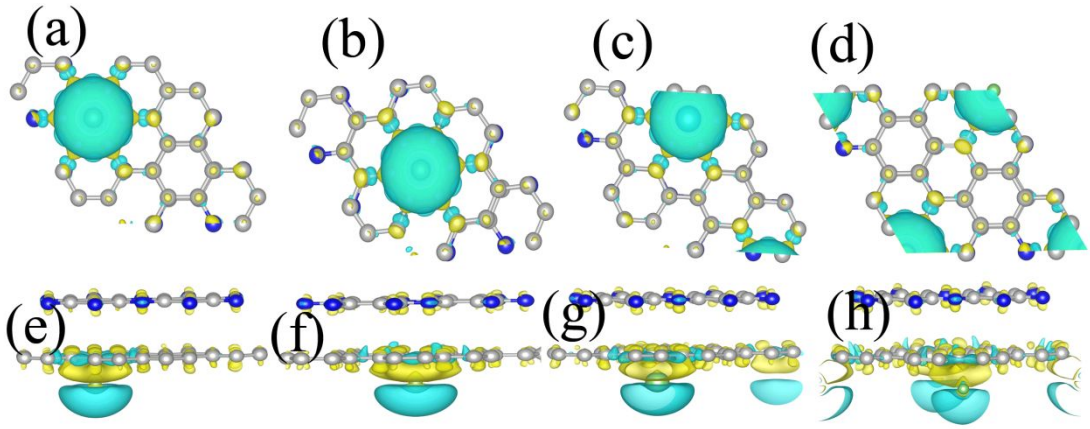

Fig. S5 The optimized structures and chosen adsorption sites (bottom of graphene) of AA stacking for monolayer C_2N/G heterostructures. The charge density difference, (bottom and side views) of Li-middle adsorption of C_2N/G heterostructure of AA stacking. The adsorbed in G1 (a, e),G2 (b, f), G3 (c, g) and G4 (d, h).

Table S1 The calculated adsorption energy (E_{ad} , eV) C_2N/G heterostructure using the spin non-polarized methods and spin polarized.

		spin non-polarized	spin polarized
AA	site	Adsorption energy	Adsorption energy
Up	CN1	0.1551	0.1404
	CN2	-0.0563	-0.076
	CN3	-2.9637	-2.9803
	CN4	-2.9805	-3.0003
Middle	GCN1	-0.3078	-0.3277
	GCN2	-0.4940	-0.5057
	GCN3	-2.9640	-2.9807
Down	G1	0.3111	0.2901
	G2	0.3041	0.2834
	G3	0.3025	0.2810

Table S2The calculated adsorption energy (E_{ad} , eV) value at difference sites

C_2N/G heterostructure						~~Graphene~~		~~C_2N~~	
AA	site	Adsorption energy	AB	site	Adsorption energy	site	Adsorption energy	site	Adsorption energy
Up	CN1	0.1551	Up	CN1	-3.0713	CN1	0.1475	G1	0.5301
	CN2	-0.0563		CN2	-0.1667	CN2	-0.0858	G2	0.5301
	CN3	-2.9637		CN3	0.0639	CN3	-2.9027	G3	0.5300
	CN4	-2.9805							
Middle	GCN1	-0.3078	Middle	GCN1	-3.0889				
	GCN2	-0.4940		GCN2	-0.4682				
	GCN3	-2.9640		GCN3	-0.2459				
Down	G1	0.3111	Down	D_1	0.2138	CN1	0.1475	G1	0.5301
	G2	0.3041		D_2	0.1913	CN2	-0.0857	G2	0.5301
	G3	0.3025		D_3	0.2236	CN3	-2.9188	G3	0.5301

Table S3 Calculated diffusion barriers (E_a , eV) along different paths.

		Up_1-Up_2	Up_1-Up_3	Up_2-Up_3	Mid_1-Mid_2	Mid_1-Mid_3	Mid_2-Mid_3	$Down_1$-$Down_2$	$Down_1$-$Down_3$	$Down_3$-$Down_4$	Up_{13}-Up_{23}	Mid_{13}-Mid_{23}
C_2N/G heterostructure	AA	0.14	0.13	0.06	0.17	0.02	0.06	0.30	0.30	0.30	0.14	0.22
	AB	2.96	3.23	0.36	2.61	2.82	0.03	0.30	0.30	0.30	2.28	1.53
C_2N		0.14	0.10	0.06								
Graphene		0.31	0.31	0.31								
VS_2/G heterostructure	[28]					0.2	0.2					
MoS_2/G heterostructure	[44]				0.17	0.23	0.10					
Si/G heterostructure	[45]	0.36			0.37			0.40				
G/blue-phosphorus heterostructure	[46]				0.23	0.22						
P/G heterostructure	[35]	0.09			0.12	0.79		0.25				
G/metal sulfide(MoS2/G)	[49]				0.18							
G/metal sulfide(SnS_2/G)	[49]				0.21							

(28) Mikhaleva, N. S.; Visotin, M.; Kuzubov, A. A.; Popov, Z. I. VS_2/Graphene heterostructures as promising anode material for Li-ion batteries. *J. Phys. Chem. C*, **2017**, 121, 24179–24184.

(30) Wang, L.; Jiang, Z.; Li, W.; Gu, X.; Huang, L. Hybrid phosphorene/grapheme nanocomposite as an anode material for Na-ion batteries: a first-principles study. *J. Phys. D: Appl. Phys.* **2017**, 50, 165501.

(39) Miwa1, R. H.; Scopel, W. L. Lithium incorporation at the MoS_2/graphene interface: an ab initio investigation. J. *phys. Cond. matt.***2013**, 25, 445301-445305.

(45) Shi, L.; Zhao, T. S.; Xu, A.; Xu, J. B. Ab initio prediction of a silicene and graphene heterostructure as an anode material for Li-and Na-ion batteries. *J.Mater. Chem. A* **2016**, 4, 16377-16382.

(46) Fan, K.; Tang, J.; Wu, S.; Yang, C.; Hao, J.; Adsorption and diffusion of lithium in a graphene/blue-phosphorus heterostructure and the effect of an external electric field. *Phys. Chem. Chem. Phys.*

2017, 19, 267-275.
(49) Lv, Y.; Chen, B.; Zhao, N.; Shi, C.; He, C.; Li, J.; Liu. E.; Interfacial effect on the electrochemical properties of the layered graphene/metal sulfide composites as anode materials for Li-ion batteries. *Surf. Sci*. **2016**, 651, 10-15.

Table S4 Bader charge and charger transfer for lithium adsorbed at the middle of C_2N/G heterostructure with AA stacking.

	atom	GCN1	GCN2	GCN3		GCN1	GCN2	GCN3		atom	GCN1	GCN2	GCN3		GCN1	GCN2	GCN3
						ΔQ	Δ Q	Δ Q							Δ Q	Δ Q	Δ Q
	C1	3.9481	3.944	3.961	4	-0.0519	-0.056	-0.039		C25	3.5093	3.4848	3.471	4	-0.4907	-0.5152	-0.529
	C2	3.9356	3.9459	3.9505	4	-0.0644	-0.0541	-0.0495		C26	3.5499	3.4657	3.4766	4	-0.4501	-0.5343	-0.5234
	C3	4.0644	3.9402	3.9547	4	0.0644	-0.0598	-0.0453		C27	3.5607	3.5819	3.5457	4	-0.4393	-0.4181	-0.4543
	C4	4.034	4.0443	4.0476	4	0.034	0.0443	0.0476		C28	3.4552	3.5039	3.4958	4	-0.5448	-0.4961	-0.5042
	C5	4.0554	4.0451	4.0544	4	0.0554	0.0451	0.0544		C29	3.4693	3.4346	3.5662	4	-0.5307	-0.5654	-0.4338
	C6	4.1103	4.0536	4.0563	4	0.1103	0.0536	0.0563		C30	3.4507	3.5225	3.5105	4	-0.5493	-0.4775	-0.4895
	C7	4.0529	3.9482	3.956	4	0.0529	-0.0518	-0.044		C31	3.4406	3.4959	3.4682	4	-0.5594	-0.5041	-0.5318
	C8	3.9966	4.0002	3.9556	4	-0.0034	0.0002	-0.0444		C32	3.4612	3.4522	3.4858	4	-0.5388	-0.5478	-0.5142
	C9	3.9466	4.0016	3.9566	4	-0.0534	0.0016	-0.0434		C33	3.476	3.5897	3.4746	4	-0.524	-0.4103	-0.5254
	C10	4.0878	4.0414	4.056	4	0.0878	0.0414	0.056	up	C34	3.5659	3.5035	3.5086	4	-0.4341	-0.4965	-0.4914
	C11	4.0954	4.1043	4.0555	4	0.0954	0.1043	0.0555		C35	3.5604	3.4471	3.5179	4	-0.4396	-0.5529	-0.4821
down	C12	4.0336	4.085	4.0486	4	0.0336	0.085	0.0486		C36	3.559	3.5208	3.4586	4	-0.441	-0.4792	-0.5414
	C13	3.9552	3.947	3.9568	4	-0.0448	-0.053	-0.0432		C_{sum}					-5.9418	-5.9974	-6.0205
	C14	3.9472	3.9391	3.9529	4	-0.0528	-0.0609	-0.0471		N1	6.0817	6.1143	6.1971	5	1.0817	1.1143	1.1971
	C15	3.9435	3.9376	3.944	4	-0.0565	-0.0624	-0.056		N2	6.0843	6.1418	6.1075	5	1.0843	1.1418	1.1075
	C16	3.9711	4.0457	4.0472	4	-0.0289	0.0457	0.0472		N3	6.1176	6.1209	6.0804	5	1.1176	1.1209	1.0804
	C17	4.0499	4.0439	4.0534	4	0.0499	0.0439	0.0534		N4	6.0775	6.0822	6.186	5	1.0775	1.0822	1.186
	C18	3.9693	3.9836	4.046	4	-0.0307	-0.0164	0.046		N5	6.1312	6.1272	6.1293	5	1.1312	1.1272	1.1293
	C19	4.0077	4.0477	3.9476	4	0.0077	0.0477	-0.0524		N6	6.104	6.0746	6.157	5	1.104	1.0746	1.157
	C20	3.9522	3.9369	3.9531	4	-0.0478	-0.0631	-0.0469		N_{sum}					6.5963	6.6610	6.8573
	C21	3.9475	3.9483	3.9548	4	-0.0525	-0.0517	-0.0452		Up_{sum}					0.6545	0.6636	0.8368
	C22	4.0549	4.1116	4.0573	4	0.0549	0.1116	0.0573									
	C23	3.9836	4.0453	4.0519	4	-0.0164	0.0453	0.0519									
	C24	4.0571	4.0521	4.056	4	0.0571	0.0521	0.056									
	$Down_{sun}$					0.1999	0.1926	0.0738	mid	Li1	0.1457	0.1438	0.0896	1	-0.8543	-0.8562	-0.9104